Synthesis, Structural Characterization and Spectroscopic Properties of 1,2-Bis[4-(3,5-dimethyl-1*H*-pyrazol-1-yl)-2-oxobutyl]benzene

Miguel Guerrero • Josefina Pons • Mercè Font-Bardia •Teresa Calvet • Josep Ros

M. Guerrero • J. Pons (&) • J. Ros, Departament de Química, Unitat de Química Inorgànica, Facultat de Ciències, Universitat Autònoma de Barcelona, Bellaterra-Cerdanyola, 08193 Barcelona, Spain

e-mail: Josefina.Pons@uab.es

M. Font-Bardia • T. Calvet. Cristal lografia, Mineralogia i Dipòsits Minerals, Universitat de Barcelona, Martí i Franquès s/n, 08028 Barcelona, Spain

Abstract

The crystal structure of the title compound $C_{22}H_{30}N_4O_2 \cdot H_2O$ (**L**), has been determined using X-ray diffraction at 293 K. The crystal of 1,2-bis[4-(3,5-dimethyl-1H-pyrazol-1-yl)-2-oxobutyl]benzene is in triclinic crystal system with space group P(-1) (Z = 2), lattice parameters a = 8.225(6) Å , b= 10.967(6) Å , c= 12.903(6) Å, V = 1119.1(11) Å 3. Analyses of single crystals of **L**, crystallized from dichloromethane/diethyl ether (1:1), revealed that the molecules are arranged in couples, which adopt a pseudo chair conformation, by means of intermolecular O–H···N hydrogen bonding interactions. Moreover, the extended structure revealed a 1D chain caused by several C–H···N intermolecular interactions.

1. INTRODUCTION

Since the first comprehensive review of pyrazole derived ligands appeared in 1972 [1], the preparation and characterization of pyrazole and its derivatives have been developed vigorously over the last three decades [2–5]. Moreover, the recent period has evidenced an everincreasing interest in pyrazole-based hybrid ligands containing hard and soft donor atoms. This kind of ligands has been extensively used in coordination and organometallic chemistry due to their ability to provide an extensive variety of coordination geometries and significant structural nuclearity introducing different kinds of heteroatoms [6–8]. The combination of coordination chemistry with intermolecular interactions, provides a powerful method for creating supramolecular architectures from simple building blocks [9, 10].

In the last 10 years our research group has focused on the synthesis and characterization of the *N*-hydroxyalkylpyrazole, *N*-hydroxyalkyl-3,5-dimethylpyrazole and *N*-hydroxyalkylpyridylpyrazole ligands [11–15]. Recently, we have been interested in the design of new systems of *N*-pyrazolether and exploring their ability as potential host molecules for future industrial applications [16–20].

In this paper, we present the synthesis and the solid state structure analyses of 1,2-bis[4-(3,5-dimethyl-1*H*-pyrazol-1-yl)-2-oxobutyl]benzene (L) (Scheme 1). The molecules in the crystal packing are arranged in couples, across inversion centres, by means of weak intermolecular O–H⋯N and C–H⋯N bonding interactions.

2. EXPERIMENTAL SECTION

Materials and Measurements

The reactions were carried out under nitrogen atmosphere using vacuum line and Schlenk techniques. All solvents were dried and distilled according to standard procedures and stored under nitrogen [21]. Crystals of title compound (**L**), suitable for X-ray diffraction, were obtained by slow evaporation of a solution in dichloromethane/diethyl ether (1:1) at 293 K. The data were collected using a MAR345 diffractometer with a image plate detector. Unit-cell parameters were determined from 121 reflections ($3 < \theta < 31°$) and refined by least-squares method. Intensities were collected with graphite monochromatized Mo Kα radiation. 11,349 reflections were measured in the range $1.60 \leq \theta \leq 32.29°$, 6,119 of which were non-equivalent by symmetry (R_{int}(on I) = 0.030). 4,135 reflections were assumed as observed applying the condition $I > 2\sigma(I)$. Lorentz-polarization but no absorption corrections were made.

The structure was solved by Direct methods, using SHELXS97 computer program [22], and refined by fullmatrix least-squares method with SHELXL97 computer program [23] using 11,349 reflections, (very negative intensities were not assumed). The function minimized was $\sum w \left| \left|F_O\right|^2 - \left|F_C\right|^2 \right|^2$ where $x = [\sigma^2(I) + (0.0934P)^2]^{-1}$, and $P = (\left|F_O\right|^2 + 2\left|F_C\right|^2)/3$. 2 H atoms were located from a difference synthesis and were refined with an isotropic temperature factor and 30 H atoms were computed and refined, using a riding model, with an isotropic temperature factor equal to 1.2 time the equivalent temperature factor of the atom which are linked. Table 1 illustrates the crystal data and structure refinements of **L**.

Melting point was measured on a Electro-thermal 1A8104 melting point apparatus. Elemental analyses (C, H, N) were carried out by the staff of Chemical Analyses Service of the Universitat Autònoma de Barcelona on a Carlo Erba CHNS EA-1108 instrument. Infrared spectra were run on a Perkin-Elmer FT spectrophotometer, series 2,000 cm^{-1} as KBr pellets or polyethylene films in the range 4,000–600 cm^{-1}. ^{1}H, ^{13}C{^{1}H}, and HMQC spectra were recorded on an NMR-FT Bruker AC-250 MHz spectrometer in [D]chloroform solution at room temperature. All chemical shifts values (δ) are given in ppm. Mass spectrum was obtained with an Esquire 3000 ion trap mass spectrometer from Bruker Daltonics.

Synthesis of $C_{22}H_{30}N_4O_2 \cdot H_2O$ (**L**)

97   A solution of 2.80 g (0.020 mol) of 1-(2-hydroxyethyl)-3,5-dimethylpyrazole [24] in

98 50 mL of tetrahydrofuran was slowly added to a suspension of 0.53 g (0.022 mol) of NaH in

99 10 mL of tetrahydrofuran. The solution was stirred at 60 °C for 2 h. 2.75 g (0.010 mol) of

100 α,α'-dibromo-*o*-xylene in 10 mL of tetrahydrofuran were the added dropwise and under

101 vigorous stirring. The resulting mixture was allowed to stir for 12 h at 60 °C. After cooling

102 to room temperature, 10 mL of water were added dropwise in order to destroy excess NaH.

103 The solvents were then evaporated under reduced pressure. The residue was taken up in

104 water (40 mL) and extracted with chloroform (3 x 50 mL). The chloroform layers were dried

105 with anhydrous $MgSO_4$ and evaporated. The crystals were obtained by the slow evaporation

106 of a solution in dichloromethane/diethyl ether (1:1) at 293 K.

107   Yield: 2.60 g (65%). Mp: 68.7–69.9 °C. $(C_{22}H_{30}N_4O_2 \cdot H_2O)$: Anal. Calc.: C, 65.98;

108 H, 8.05; N, 13.99; Found: C, 65.72; H, 7.94; N, 13.67%. MS(ESI): m/z (%) = 383 (100) [L

109 + H]$^+$. IR (KBr, cm^{-1}): 3,454 ν (O–H), 3,129 ν (C–H)$_{ar}$, 2,986, 2,865 ν (C–H)$_{al}$, 1,623 d(O–

110 H), 1,556 (ν (C=C), ν(C=N))$_{ar}$, 1,422 (δ(C=C), δ (C=N))$_{ar}$, 1,104 ν (C–O–C), 754 δ (C–

111 H)$_{oop}$. ^{1}H NMR ([D]chloroform solution, 250 MHz) δ: 7.21 [4H, br, Ph], 5.81 [2H, s,

112 CH(pz), 4.40 [4H, s, OCH$_2$Ph], 4.15 [4H, t, ^3J = 5.8 Hz, NpzCH$_2$ CH$_2$O], 3.68 [4H, t, ^3J =

113 5.8 Hz, NpzCH$_2$CH$_2$O], 2.28 [s, 12H, CH$_3$(pz)] ppm. ^{13}C{^{1}H} NMR ([D]chloroform

114 solution, 63 MHz,) δ: 147.5 (pz-C), 140.3 (pz-C), 136.9-128.5 (Ph), 105.9 (CH(pz)), 73.7

115 (OCH$_2$Ph), 69.1 (NpzCH$_2$ CH$_2$O), 49.2 (NpzCH$_2$CH$_2$O), 12.5 (CH$_3$(pz)), 11.4 (CH$_3$(pz))

116 ppm.

117

118

119

3. RESULT AND DISCUSSION

120

121   The synthetic route for the preparation of the ligand 1,2-bis[4-(3,5-dimethyl-1H-

122 pyrazol-1-yl)-2-oxobutyl]benzene (**L**) consists of two steps (Scheme 1). The 1-(2-

123 hydroxyethyl)-3,5-dimethylpyrazole was reacted with NaH in dry tetrahydrofuran to give

124 the sodium alkoxide. This sodium salt was converted to ligand **L**, by reacting it with α, α'-

125 dibromo-*o*-xylene in dry tetrahydrofuran. For **L** it has been possible to obtain colourless

126 monocrystals suitable for X-ray analysis through crystallization from a

127 dichloromethane/diethyl ether (1:1) mixture.

128   The ligand has been fully characterized by melting point, elemental analysis, mass

129 spectrometry, IR, ^{1}H, ^{13}C{^{1}H} NMR spectroscopies and X-ray crystal structure. The NMR

130 signals were assigned by reference to the literature [25] and from COSY and HMQC NMR

131 experiments. Elemental analysis, mass spectrometry and all spectroscopic data are consistent

132 with the proposed structure. The most characteristic bands in the IR spectra are those

133 attributable to the ether (ν(C–O–C)) and pyrazolyl groups (ν (C=C), ν (C=N), δ(C–H)$_{oop}$)

134 [25]. A strong and welldefined band at 3,454 cm^{-1} it is also observed, which corresponds to

135 ν (O–H) and it is generally associated to coordinated water molecules [26]. In the NMR, at

136 room temperature, the signals attributable to CH group of the pyrazole ring appear at (δ(^{1}H)

137 = 5.81 and δ(^{13}C{^{1}H}) = 105.9 ppm).

138   The ORTEP [27] view of compound **L** is shown in Fig. 1. Selected bond lengths and

139 bond angles are presented in Table 2. The crystal structure, which lies on a crystallographic

140 inversion centre, consists of one dimeric molecule formed by two ligands and two molecules

141 of water (Fig. 2). The two potentially active **H** atoms (water molecules) are engaged in

142 intermolecular bonds with the lone-pair of the **N** atom of the pyrazolyl group of **L**, which

143 acts as a bidentate bridge ligand. Each pair of pyrazole rings of the molecule **L** are almost

144 perpendicular to each other (interplanar angle of 77(9)°) and one of them coplanar to the

145 benzene groups (interplanar angle of 4(1) °). The distance between two consecutive oxygen

146 atoms (OW1) in the macrocycle is 14.483(4) Å . Moreover, the aromatic rings are parallel

147 planar but do not overlap (their centroids are displaced by over 4 Å), and therefore exhibit

148 evidence of very slight intramolecular π–π interaction in the solid state. However, in this

149 system, the free ether moieties can be envisaged to be applied in host–guest chemistry
150 because of the similarity with the hetero-crown ether [28, 29].

151   A detailed examination of the crystal packing (Fig. 3) revealed that each dimeric unit
152 is linked to two neighbouring molecules, which all are in the same plane, via four C–H···N
153 intermolecular bonding (2.721(2) Å). This intermolecular interaction leads to the formation
154 of a one dimensional infinite chain, running approximately along the b axis. The X–H···N
155 (X = C or O) intermolecular contacts can be considered as ''weak'' on the basis of the contact
156 distances and angles reported by Steiner [30]. The details of the hydrogen bonding
157 interactions are given in Table 3.

158

159

160

161

162

CONCLUSION

In summary, we have synthesized the 1,2-bis[4-(3,5-dimethyl-1*H*-pyrazol-1-yl)-2-oxobutyl]benzene (**L**) ligand. The X-ray analysis reveals that **L** adopts a pseudo chair conformation. The ligand is arranged in couples by means of intermolecular O–H⋯N hydrogen bonding interactions. The extended structure shows a 1D chain caused by several weak C–H⋯N intermolecular interactions.

ACKNOWLEDGEMENTS

6. REFERENCES

1. Trofimenko S (1972) Chem Rev 72:497–508

2. Pettinari C, Pettinari R (2005) Coord Chem Rev 249:663–691

3. La Monica G, Ardizzoia GA (1997) Prog Inorg Chem 46:151–213

4. Trofimenko S (1993) Chem Rev 93:943–980

5. Trofimenko S (1986) Prog Inorg Chem 34:115–210

6. Klingele J, Dechert S, Meyer F (2009) Coord Chem Rev 253:2698–2741

7. Halcrow MA (2009) Dalton Trans 2059–2073

8. Mukherjee R (2000) Coord Chem Rev 203:151–218

9. Desiraju GR (2002) Acc Chem Res 35:565–573

10. Piguet C, Bernardinelli G, Hopfgartner G (1997) Chem Rev 97:2005–2062

11. Boixassa A, Pons J, Solans X, Font- M, Ros J (2003) Inorg Chim Acta 355:254–263

12. Boixassa A, Pons J, Solans X, Font-Bardía M, Ros J (2004) Inorg Chim Acta 357:733–738

13. Boixassa A, Pons J, Virgili A, Solans X, Font-Bardía M, Ros J (2002) Inorg Chim Acta 340:49–55

14. Montoya V, Pons J, Branchadell V, García-Antón J, Solans X, Font-Bardía M, Ros J (2008) Organometallics 27:1084–1091

15. Montoya V, Pons J, García-Antón J, Solans X, Font-Bardía M, Ros J (2007) Inorg Chim Acta 360:625–637

16. Boixassa A, Pons J, Solans X, Font-Bardía M, Ros J (2003) Inorg Chim Acta 346:151–157

17. Boixassa A, Pons J, Ros J, Mathieu R, Lugan N (2003) J Organomet Chem 682:233–239

18. Boixassa A, Pons J, Solans X, Font-Bardía M, Ros J (2004) Inorg Chim Acta 357:827–833

219 19. Guerrero M, Pons J, Branchadell V, Parella T, Solans X, Font-Bardía M, Ros J (2008)
220   Inorg Chem 47:11084–11094

221 20. Guerrero M, Pons J, Parella T, Font-Bardía M, Calvet T, Ros J (2009) Inorg Chem
222   48:8736–8750

223 21. Armarego WLF, Perrin D (1996) Purification of laboratory chemicals. Butterworth-
224   Heinemann, Oxford

225 22. Sheldrick GM (1997) SHELXS-97, program for crystal structure determination.
226   University of Göttingen, Germany

227 23. Sheldrick GM (2008) Acta Cryst A64:112–122

228 24. Haanstra WG, Driessen WL, Reedijk J, Turpeinen U, Hämäläinen R (1989) J Chem
229   Soc Dalton Trans 11:2309–2314

230 25. Williams DH, Fleming I (1995) Spectroscopic methods in organic chemistry.
231   McGraw-Hill, London

232 26. Pretsh E, Clerc T, Seibl J, Simon W (1989) Tables of determination of organic
233   compounds. 13C NMR, 1H NMR, IR, MS, UV/Vis. Chemical Laboratory Practice,
234   Berlin

235 27. Burnett MN, Johnson CK (1996) ORTEP III, report ORNL-6895. Oak Ridge National
236   Laboratory, Oak Ridge

237 28. Tsubuke H (1996) Coord Chem Rev 148:1–17

238 29. Schäfer M (2003) Angew Chem Int Ed 42:1896–1899

239 30. Steiner T (2002) Angew Chem Int Ed 41:48–76

240

241

242

243   **Table 1** Crystal data and refinement parameters for the compound $C_{22}H_{30}N_4O_2\cdot H_2O$ (**L**)

244

CCDC	771079
Molecular formula	$C_{22}H_{32}N_4O_3$
Molecular weight	400.52
Temperature (K)	293(2)
Crystal system	Triclinic
Space group	P(−1)
a (Å)	8.225(6)
b (Å)	10.967(6)
c (Å)	12.903(6)
α (°)	92.09(3)
β (°)	98.44(3)
γ (°)	102.94(3)
V (Å^3)	1119.1(11)
Z	2
D_{calc} (g cm^{-3})	1.189
Absorption coefficient (mm^{-1})	0.080
$F(000)$	432
Radiation (λ)	MoKα (0.71073 Å)
Crystal dimensions (mm)	0.2 × 0.09 × 0.09
θ range (°)	1.60–32.29
Index range	−12 ≤ h ≤ 11, −16 ≤ k ≤ 16, −19 ≤ l ≤ 19
Reflections collected/unique	11349/6119 [R(int) = 0.0308]
Completeness to θ (%)	93.4
Absorption correction	Empirical
Max. and min. transmission	0.99 and 0.98
Data/restraints/parameters	6119/14/271
Goodness-of-fit	1.082
Final R_1, ωR_2	0.0497, 0.1483
R_1 (all data), ωR_2	0.0784, 0.1703
Largest diff. peak and hole	0.230 and −0.215

245

246

247   **Table 2.** Selected bond lengths (Å), bond angles (°) and torsion angles (°) for the compound

248    $C_{22}H_{30}N_4O_2 \cdot H_2O$ (**L**)

Bond lengths	
O(1)–C(7)	1.4129(18)
O(1)–C(8)	1.4331(18)
O(2)–C(15)	1.4109(16)
O(2)–C(16)	1.4161(17)
N(1)–N(2)	1.3608(16)
N(1)–C(1)	1.364(2)
N(1)–C(6)	1.442(2)
N(2)–C(3)	1.334(2)
N(3)–C(18)	1.3476(19)
N(3)–N(4)	1.3614(19)
N(3)–C(17)	1.453(2)
N(4)–C(20)	1.333(2)
C(1)–C(2)	1.373(2)
C(1)–C(4)	1.484(2)
C(2)–C(3)	1.393(2)
C(3)–C(5)	1.492(2)
C(6)–C(7)	1.503(2)
C(8)–C(9)	1.499(2)
C(9)–C(10)	1.386(2)
C(9)–C(14)	1.4064(18)
C(10)–C(11)	1.376(3)
C(11)–C(12)	1.381(3)
C(12)–C(13)	1.387(2)
C(13)–C(14)	1.381(2)
C(14)–C(15)	1.5150(19)
C(16)–C(17)	1.509(2)
C(18)–C(19)	1.375(2)
C(18)–C(22)	1.489(2)
C(19)–C(20)	1.395(2)
C(20)–C(21)	1.504(3)
Bond angles	
C(7)–O(1)–C(8)	112.91(11)
C(15)–O(2)–C(16)	111.35(11)
N(2)–N(1)–C(1)	112.15(12)
N(2)–N(1)–C(6)	119.31(12)
C(1)–N(1)–C(6)	128.43(13)
C(3)–N(2)–N(1)	104.87(12)
C(18)–N(3)–N(4)	112.70(12)
C(18)–N(3)–C(17)	128.36(13)
N(4)–N(3)–C(17)	118.88(12)
C(20)–N(4)–N(3)	104.59(12)
N(1)–C(1)–C(2)	105.55(14)
N(1)–C(1)–C(4)	123.55(16)
C(2)–C(1)–C(4)	130.90(16)
C(1)–C(2)–C(3)	106.57(15)
N(2)–N(3)–C(2)	110.85(13)
N(2)–C(3)–C(5)	119.95(14)
C(2)–C(3)–C(5)	129.19(15)

249

250

251

252

253   **Table 2.** continued

N(1)–C(6)–C(17)	113.05(13)
O(1)–C(7)–C(6)	108.62(13)
O(1)–C(8)–C(9)	112.33(12)
C(10)–C(9)–C(14)	118.60(14)
C(10)–C(9)–C(8)	120.54(13)
C(14)–C(9)–C(8)	120.85(12)
C(11)–C(10)–C(9)	121.94(15)
C(10)–C(11)–C(12)	119.23(16)
C(11)–C(12)–C(13)	119.88(17)
C(14)–C(13)–C(12)	121.07(15)
C(13)–C(14)–C(9)	119.24(13)
C(13)–C(14)–C(15)	121.47(13)
C(9)–C(14)–C(15)	119.27(12)
O(2)–C(15)–C(14)	110.42(11)
O(2)–C(16)–C(17)	109.54(12)
N(3)–C(17)–C(16)	113.80(11)
N(3)–C(18)–C(19)	105.61(13)
N(3)–C(18)–C(22)	123.88(14)
C(19)–C(18)–C(22)	130.49(15)
C(18)–C(19)–C(20)	106.41(14)
N(4)–C(20)–C(19)	110.68(14)
N(4)–C(20)–C(21)	120.97(15)
C(19)–C(20)–C(21)	128.35(16)
Torsion angles	
N2–N1–C6–C7	76.61
N4–N3–C17–C16	76.58
C9–C8–O1–C7	−79.96
C14–C15–O2–C16	172.16
C8–C9–C14–C15	−3.17

254

255

256

257

258   **Table 3.** Distances (d, Å) and angles ($\angle$, °) related to hydrogen bonding in the compound

259    $C_{22}H_{30}N_4O_2 \cdot H_2O$ (**L**)

	d (D–H)	d (H$\cdots$A)	d (D$\cdots$A)	$\angle$(D$\cdots$A)	Symmetry code
O (1W)–H (1W)$\cdots$N (2)	0.901 (15)	2.199 (14)	2.998 (3)	148 (2)	x, 1 + y, z
O (1W)–H (2W)$\cdots$N (4)	0.900 (12)	2.41 (2)	3.008 (3)	124 (18)	2 − x, 1 − y, 1 − z
C (22)–H (22A)$\cdots$N (2)	0.959 (12)	2.72 (3)	3.527 (3)	142 (18)	1 + x, y, z

260

261

262

263

264

265

266

Figures Captions

Scheme 1. Synthesis of the ligand (**L**)

Figure 1. ORTEP diagram of ligand **L** showing atom labelling scheme. 50% probability amplitude displacement ellipsoids are shown. Hydrogen atoms are omitted for clarity. See Table 2 for selected bond lengths, bond angles and torsion angles

Figure 2. View of the supramolecular architecture of the **L** units generated by intermolecular O–H N bonding interactions. The hydrogen atoms have been omitted for clarity. O–H N bonding interactions are indicated with dashed lines. See Table 3 for selected bond lengths and bond angles

Figure 3. A vision of the threedimensional ordering of the **L** units. O–H$\cdots$N bonding interactions are indicated with dashed lines

279   **Scheme 1**
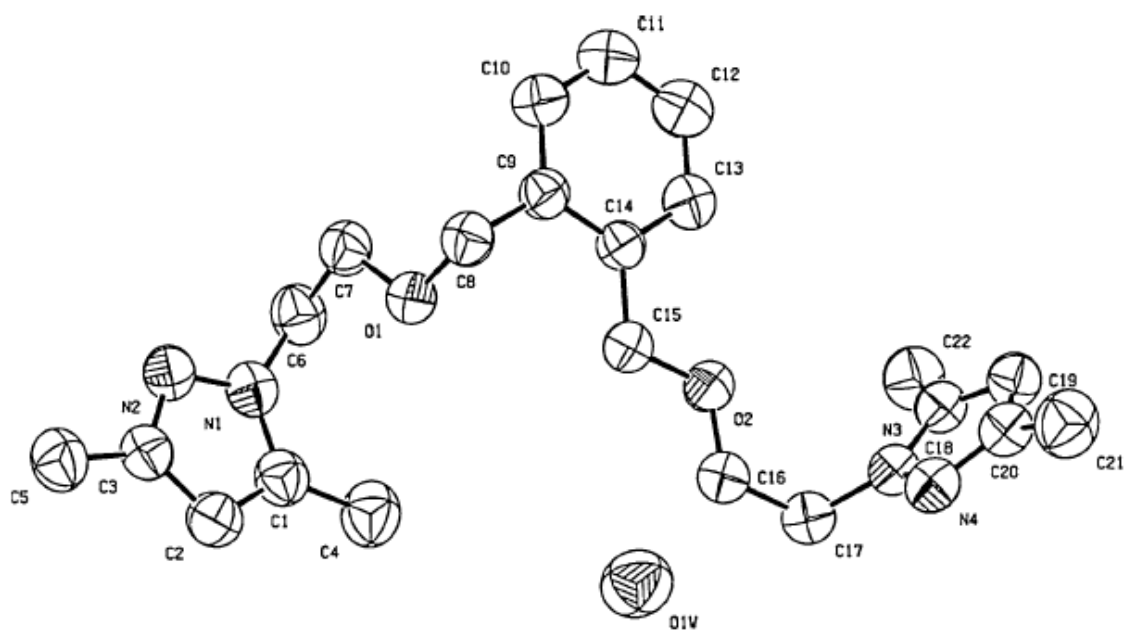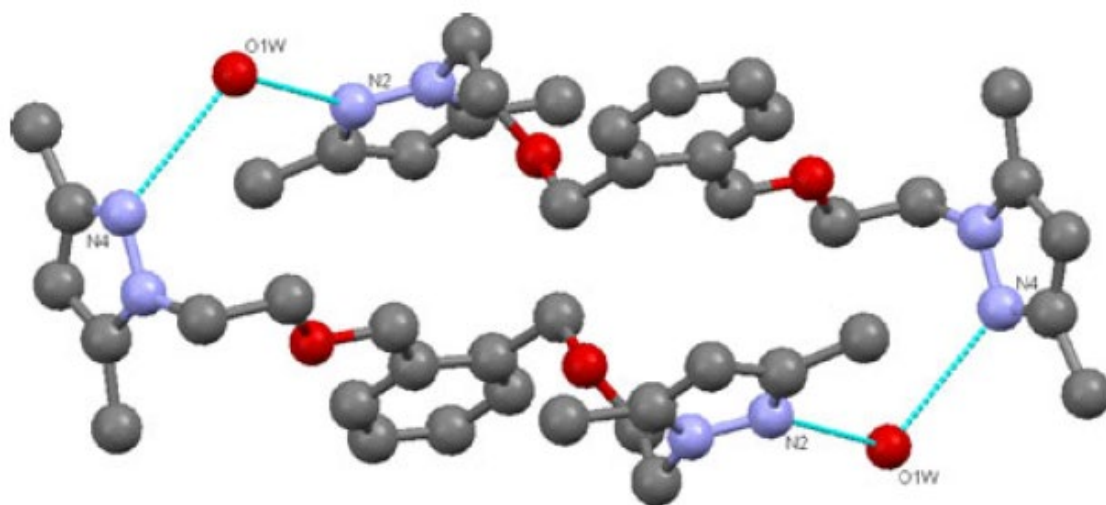
280
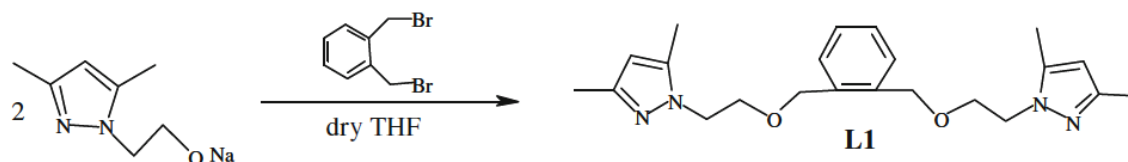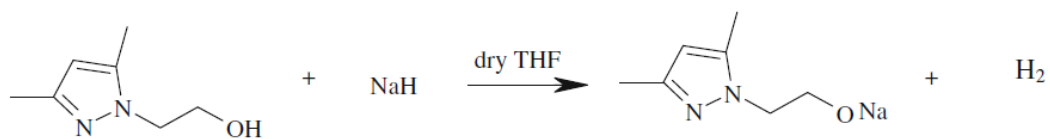
281

282

283

284

285   **Figure 1**

286

287

288

289

290

291   **Figure 2**

292

293
294
295

296   **Figure 3**

297

298

299